# Recovering signals of ghost archaic admixture in the genomes of present-day Africans

Arun Durvasula[1] and Sriram Sankararaman[1,2,3,4]

[1]Department of Human Genetics, David Geffen School of Medicine, University of California, Los Angeles

[2]Department of Computer Science, University of California, Los Angeles

[3]Bioinformatics Interdepartmental Program, University of California, Los Angeles

[4]Lead contact

March 20, 2018

**Abstract**

Analyses of Neanderthal and Denisovan genomes have characterized multiple interbreeding events between archaic and modern human populations. While several studies have suggested the presence of deeply diverged lineages in present-day African populations, we lack methods to precisely characterize these introgression events without access to reference archaic genomes. We present a novel reference-free method that combines diverse population genetic summary statistics to identify segments of archaic ancestry in present-day individuals. Using this method, we find that $7.97 \pm 0.6\%$ of the genetic ancestry from the West African Yoruba population traces its origin to an unidentified, archaic population (FDR $\leq$20%). We find several loci that harbor archaic ancestry at elevated frequencies and that the archaic ancestry in the Yoruba is reduced near selectively constrained regions of the genome suggesting that archaic admixture has had a systematic impact on the fitness of modern human populations both within and outside of Africa.

**Running title:** Reference-free inference of archaic introgression

**Correspondence:** sriram@cs.ucla.edu

# Introduction

Admixture, the exchange of genes among previously isolated populations, is increasingly being recognized as an important force in shaping genetic variation in human populations. Analyses of large collections of genome sequences have shown that admixture events have been prevalent throughout human history [1]. Further, these studies have shown that modern human populations outside of Africa trace a small percentage of their ancestry to admixture events from populations related to archaic hominins like Neanderthals and Denisovans [1, 2, 3]. Studies of the functional impacts of this introduced DNA have suggested that Neanderthal DNA that segregates in modern humans contributes to phenotypic variation [4, 5].

Central to these studies is the problem of local archaic ancestry inference – the pinpointing of segments of an individual genome that trace their ancestry to archaic hominin populations. Methods for local archaic ancestry inference leverage various summary statistics computed from modern and ancient genomes. For example, at a given genomic locus, individuals with archaic ancestry are expected to have high sequence divergence to segments of modern human ancestry but low divergence to the archaic genome [6]. A number of summary statistics have been developed to infer archaic local ancestry [7, 8, 9]. Further, statistical models that can combine these summary statistics have also been proposed [2, 10, 11].

All of these methods are most effective in settings where reference genomes that represent genetic variation in the archaic population are available. For example, the analyses of Neanderthal [6, 10] and Denisovan admixture events [12] relied on the genome sequences from the respective archaic populations. In a number of instances, however, the archaic population is either unknown or lacks suitable reference genomes. Several recent studies have found evidence for archaic introgression in present-day African populations from an unknown archaic hominin [13, 14, 15] while analysis of the high-coverage Denisovan genome has suggested that the sequenced individual traces a small proportion of its ancestry to a highly-diverged archaic hominin [10].

One of the most widely used statistics that for identifying archaic ancestry is the S*-statistic [9], which identifies highly diverged SNPs that are in high linkage disequilibrium (LD) with each other in the present-

day population as likely to be introgressed. The S*-statistic is attractive as it can be applied even where no reference genome is available. However, the power of the S*-statistics tends to be low in the reference-free setting [3]. Further, the value of the S*-statistic depends on a number of parameters that need to be fixed in advance.

Recent studies have shown that statistical predictors that combine weakly-informative summmary statistics can obtain substantially improved accuracy on a number of population genetic problems [16, 17, 18]. We extend this idea to the setting of archaic local ancestry inference and present a statistical method, ARCHaic Introgression Explorer (ArchIE), based on a logistic regression model, that combines several population genetic summary statistics to accurately predict archaic local ancestry. The parameters of ArchIE are estimated from training data generated using coalescent simulations. We show that ArchIE obtains improved accuracy in simulations over the S*-statistic while being robust to demographic model misspecification. We apply ArchIE to the 1000 Genomes Western European (CEU) population and show that the inferred segments of archaic ancestry have an increased likelihood of being introgressed from Neanderthals without access to Neanderthal genomes. In addition, the inferred segments of archaic ancestry in Europeans recover previously seen features when using reference-based methods. Specifically, using the inferences from our method, we observe a decreased frequency of Neanderthal ancestry in regions of the genome with stronger selective constraint [19] as well as elevated frequency of Neanderthal ancestry at the *BNC2* and *OAS* loci, both of which have been previously shown to harbor Neanderthal alleles at high frequency.

Finally, we apply ArchIE to genomes from the West African Yoruba (YRI) population in the 1000 Genomes Project [20] to obtain inferences of archaic local ancestry in this population. At a precision of 0.80, 7.9% of the genomes of west African individuals, on average, is estimated to trace its ancestry to a deeply-diverged archaic population. We enumerate 258 megabases (MB) of introgressed DNA, with 2.1 MB at a high ($\geq$ 50%) frequency. We observe a decrease in the frequency of archaic ancestry in the Yoruban populations in more constrained regions of the genome, suggesting that these archaic alleles have been subject to the effects of purifying selection similar to the deleterious consequences of Neanderthal and Denisovan alleles in the modern human genetic background. On the other hand, we find several loci that harbor archaic haplotypes at elevated frequencies ($>$ 60%). These results highlight the landscape of archaic introgression

into African populations and provide insight into how modern humans evolved as a species.

# Results

## Model overview

Our method, ArchIE, aims to predict the archaic local ancestry state in a given window along an individual haploid genome. This prediction is performed using a binary logistic regression model given a set of features computed within this window. Estimating the parameters of this model requires labeled training data *i.e.*, a dataset containing pairs of features and the archaic local ancestry state for a given window along an individual genome. To this end, we simulate data under a demographic model that includes archaic introgression, label windows as archaic or not, calculate a set of features that are potentially informative of introgression, and estimate the parameters of our predictor on the resulting data (Figure 1A, Methods).

We simulate training data using a modified version of the coalescent simulator, ms [21], which allows us to track each individual's ancestry. We use the demographic model used in Sankararaman *et al.* 2014 [2]. In this model, an ancestral population splits $T_0$ generations ago forming archaic and modern human populations. The modern human population splits into two populations at $T_s$, one of which then mixes with the archaic population (referred to as the target population) while the other does not (the reference population). We simulate one haploid genome (haplotype) in the archaic population, 100 haplotypes in the target population and 100 haplotypes in the reference population. In the results below, we simulate 10,000 replicates of 50,000 base pairs each (bp), resulting in 1,000,000 training examples.

We summarize the resulting data using features that are likely to be informative of archaic admixture. Since we are interested in the probability of archaic ancestry for a given haplotype, we use features that are specific for each haplotype, *i.e.*, the focal haplotype. First, for a focal haplotype, we calculate an individual frequency spectrum (IFS), which is a vector of length $n$, the sample size of the target population. Each entry in the vector counts the number of mutations on the focal haplotype that are segregating in the target population with a specific count of derived alleles. Due to the accumulation of private mutations in the archaic population, we expect an excess of alleles segregating at frequencies close to the admixture fraction

Figure 1: (A) **Outline of the demographic model used for training ArchIE**. We simulate a population starting at size $N_0$ and splitting into archaic and modern human (MH) populations at time $T_0$. The MH population splits into an MH reference and target population of size $N_1$ and $N_2$, respectively, at time $T_s$. Then, at time $T_a$, the archaic population admixes with the target population with an association admixture proportion $m$. We use data simulated from this model to train a logistic regression classifier. (B) **Distribution of predictions for ArchIE on test data**. Haplotypes predicted to have a low probability of being archaic in origin are enriched in truly non-archaic haplotypes, while truly archaic haplotypes are enriched for higher probabilities.

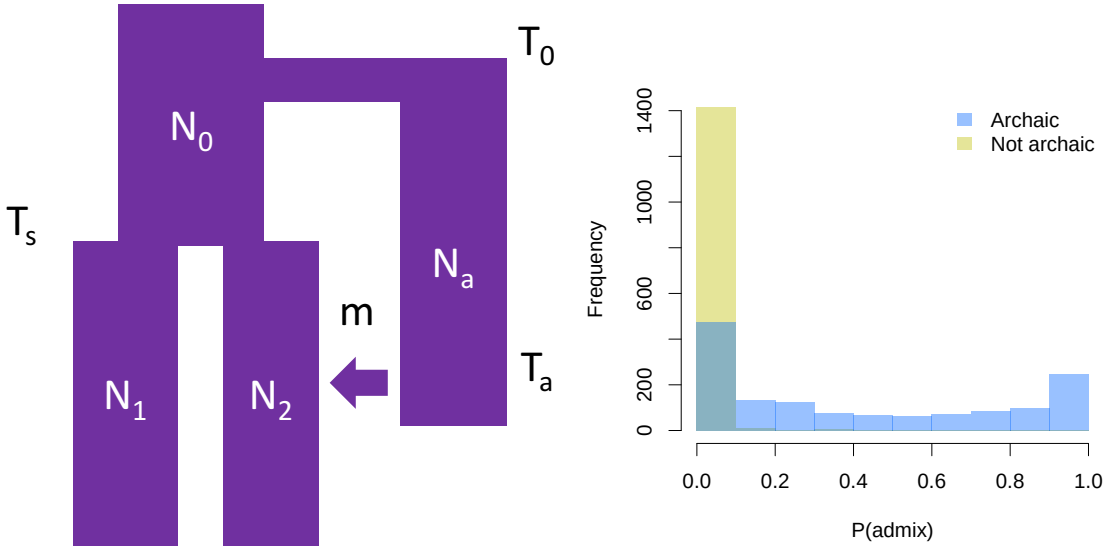

in the introgressed population. The IFS is expected to capture this signal.

Next, we calculate the Euclidean distance between the focal haplotype and all other haplotypes, resulting in a vector of length $n$. Under a scenario of archaic admixture, the distribution of pairwise differences is expected to differ when we compare two haplotypes that are both modern human or archaic versus when we compare an archaic haplotype to a modern human haplotype.

The next set of features rely on a present-day reference human population that has a different demographic history compared to the target population. We term this population the *MH reference* to make it clear that our method does not rely on an archaic reference. The choice of the MH reference will alter the specific admixture events that our method is sensitive to: we expect the method to be sensitive to admixture events in the history of the target population since its divergence from the MH reference. While our method can also be applied in the setting where no such reference population exists, in the context of human populations where genomes from a diverse set of populations is available [1], the use of the MH reference can improve the accuracy and the interpretability of our predictions. Given a reference population, we compute the minimum distance of the focal haplotype to all haplotypes in the reference population. A larger distance is suggestive of admixture from a population that diverged from the ancestor of the target and reference population before the reference and target populations split.

We also calculate the number of SNPs private to the focal haplotype, removing SNPs shared with the MH reference, as these SNPs are suggestive of an introgressed haplotype. Finally, we calculate S* [9], a feature designed for detecting archaic admixture by looking for enrichments of long stretches of derived alleles in LD.

Using these features, we train a logistic regression classifier to distinguish between archaic and non archaic segments. In our training data, we define archaic haplotypes as those that contain $\geq 70\%$ of bases with archaic ancestry and non-archaic as those that contain $\leq 30\%$ archaic ancestry. We discard haplotypes that fall in-between those values in both the training the test datasets. We simulated 1,000,000 haplotypes for the training data and 100,000 haplotypes for the test data which resulted in 988,372 training examples and 98,922 test examples after filtering. Figure 1B shows the distribution of predicted probabilities of archaic ancestry on test data. Archaic haplotypes tend to be associated with a high probability of being archaic

Figure 2: **ArchIE is more accurate than the S*-statistic** (A) Receiver Operator Characteristic (ROC) and (B) precision-recall (PR) curves for ArchIE (black crosses) and S* (red diamonds) in a 2% admixture scenario with a Human-Neanderthal demography. (C) ROC and (D) PR curves for a 20% admixture scenario.

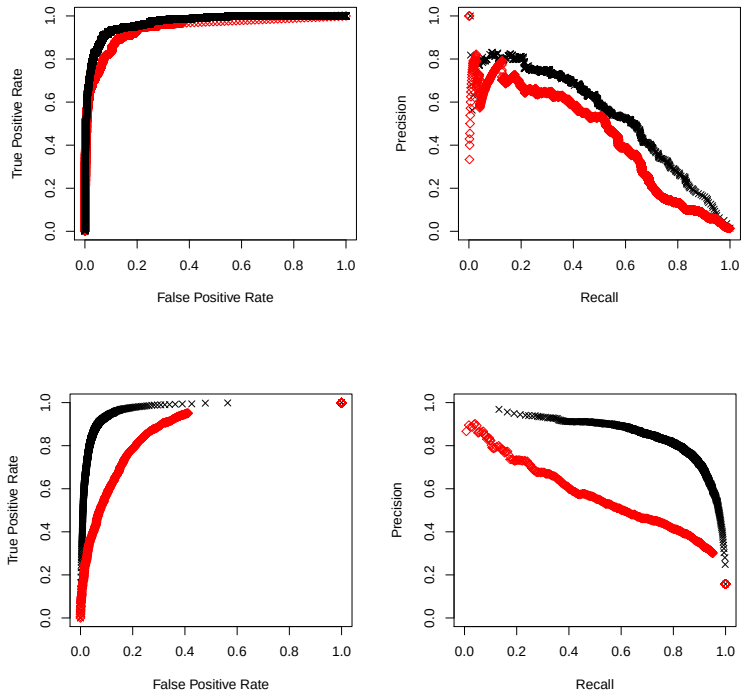


while non archaic haplotypes are enriched for low probabilities of being archaic.

## Simulation results

We tested the accuracy of ArchIE by simulating data under a demography reflective of the history of Neanderthals and present-day humans [2]. We began by simulating an admixture event with 2% Neanderthal ancestry that occurred 2,000 generations ago and simulated 1,000,000 haplotypes under 10,000 different replicates (100 haplotypes per replicate). We compute Receiver Operator Characteristic (ROC) and Precision Recall (PR) curves by varying the threshold at which we call a haplotype archaic and calculating the true positive rate (TPR), false positive rate (FPR), precision, and recall (Figure 2).

We compared these results to an implementation of the S* algorithm similar to Vernot and Akey [3]. First, we calculate S* in a cohort of 100 haplotypes from both the reference and target populations. Then,

we convert the S* scores into a rank between [0-1] using the empirical cumulative distribution. We obtain precision and recall values for varying thresholds between [0-1] and report these values. At a 2% admixture fraction, ArchIE outperforms the S* statistic across all thresholds (Figure 2AB). At a fixed precision of 0.8, *i.e.*, false discovery rate of 0.20, ArchIE obtains a recall of 0.21, while S* obtains a recall of 0.024. The area under the ROC curve is 0.943 for S* and 0.969 for ArchIE and the area under the PR curve is 0.431 for S* and 0.535 for ArchIE. We also note that while the ROC curves are quite similar, the PR curve show a large difference, indicative of the utility of PR curves in class imbalance problems.

Our simulation setup is challenging partly due to the low admixture fraction resulting in a large class imbalance across the archaic and non-archaic classes. In this setting, we find fewer than 20,000 positive examples. We compared the two methods using an admixture fraction of 20%, thereby increasing the number of positive examples in training and test data. While the accuracy of S* only slightly improved, the logistic regression classifier shows a much larger improvement (Figure 2CD). While this admixture fraction is higher than the data suggests for Human-Neanderthal introgression, it is not implausible in other species or admixture events [22, 23, 24, 25, 26, 18]. This example indicates the utility of the parameterized statistical model underlying ArchIE that can be tuned to accurately infer archaic ancestry under plausible demographic settings.

## ArchIE learns informative features

We examined the weights learned by ArchIE to understand the features that contribute substantially to its predictions. Examining single features, we find that the minimum distance between the focal haplotype and each of the reference MH haplotypes, as well as the number of private SNPs are the most positively correlated with a high probability of being archaic (Figure 3A). Intuitively, as a larger distance to a reference population and a larger number of private SNPs should both indicate archaic ancestry. The next largest single statistic was the skew of the distance vector, which was negatively correlated with archaic ancestry. Under a simple scenario of admixture, we expect a bimodal distribution of pairwise distances. However, when there is little archaic ancestry, the distribution will be skewed towards 0, resulting in a negative relationship between skew and archaic ancestry. Examining the distance vector itself, the weights are often flipped

Figure 3: **Relative importance of the features used as input to ArchIE.** We examined the weights associated with each of the features included in the logistic regression model underlying ArchIE. (A) The first four entries indicate the moments of the distance vector. The skew has the largest weight associated with it, indicating that this is the most important feature in the distance vector. The S*-statistic has a very small weight, while the minimum distance and the number of private SNPs have larger weights. (B) The distance vector has a mix of positive and negative weights, suggesting uninformative statistics. (C) The individual frequency spectrum mostly has negative weights and lower frequency entries generally have larger weights associated with them.

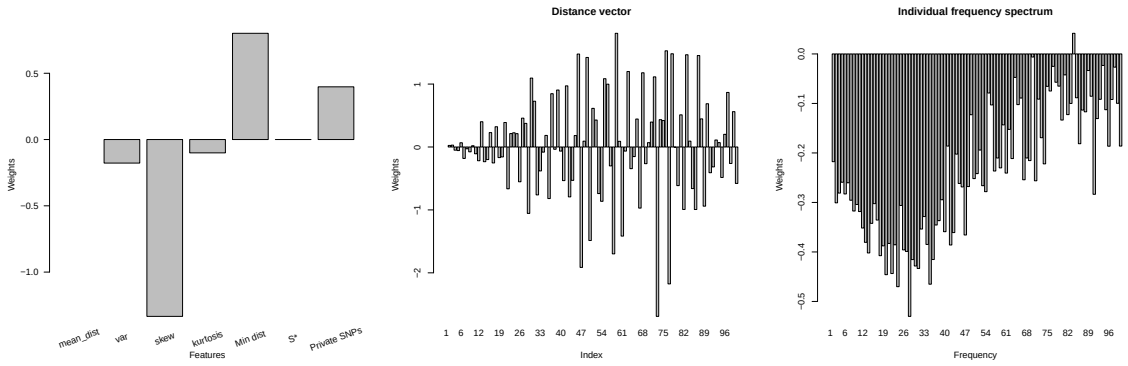

positive to negative from one entry to another (Figure 3B) suggesting there is little signal in the distance vector. On the other hand, the IFS mostly contains negative weights, suggesting that values in these entries are negatively correlated with archaic ancestry (Figure 3C). Notably, S* makes little contribution to the model likely because it is correlated with the other features included in the model.

## Classifier robustness

Our method relies on simulating data from a demography where the parameters are known. In practice, these parameters are inferred from data with some uncertainty. Thus, we wanted to determine the sensitivity of our method to demographic uncertainty. An exhaustive exploration of demographic uncertainty is challenging given the number of demographic parameters associated with even the simplest demographic models. As an alternative to an exhaustive exploration, we systematically perturbed each parameter at a time, simulated data using the perturbed model, and evaluated the performance of our classifier in terms of changes in precision and recall (trained on the unperturbed parameters corresponding to the Neanderthal demographic history).

When the parameters are not perturbed, the recall at a precision of 0.8 is 0.21 (Figure 2B). The accuracy of the classifier is unchanged or increased under many parameter changes (Figure 4). For example, increasing the split time of the modern and archaic populations ($T_0$) greatly increases the accuracy because there is more time for private mutations to accumulate on the archaic branch. Reducing this time by 25% does not result in a drop in accuracy. For time of admixture ($T_a$), decreasing the value results in improved accuracy, likely as a result of having longer haplotype blocks and less time for recombination to spread private variants across the haplotypes in the population. Decreasing the split time of the reference and target populations ($T_s$) largely leaves precision and recall the same.

Changing the population sizes of the reference ($N_1$) populations does not result in large differences in accuracy, while changing the target population size does result in decreased accuracy.

Finally, increasing the admixture fraction reduces accuracy, while decreasing it has the opposite effect. While this may seem to contradict the increased accuracy in Figure 2B when simulating a 20% admixture scenario, this is likely due to the fact that the IFS is shifted more by a 2X increase in admixture than a 0.5X

Figure 4: **ArchIE is robust to misspecification in the demographic model.** We tested ArchIE on data simulated after perturbing single demographic parameters lower (left, blue) and higher (right, orange) relative to their values in the training data. Values are reported as log fold changes compared to the baseline model performance (dashed line). We report (A, B) recall at a precision of 0.8 under different parameter misspecification scenarios. (C, D) precision at the threshold that gives a precision of 0.8 ($P(\text{archaic}) = 0.862$). (E, F) recall at the threshold that gives a precision of 0.8 ($P(\text{archaic}) = 0.862$).

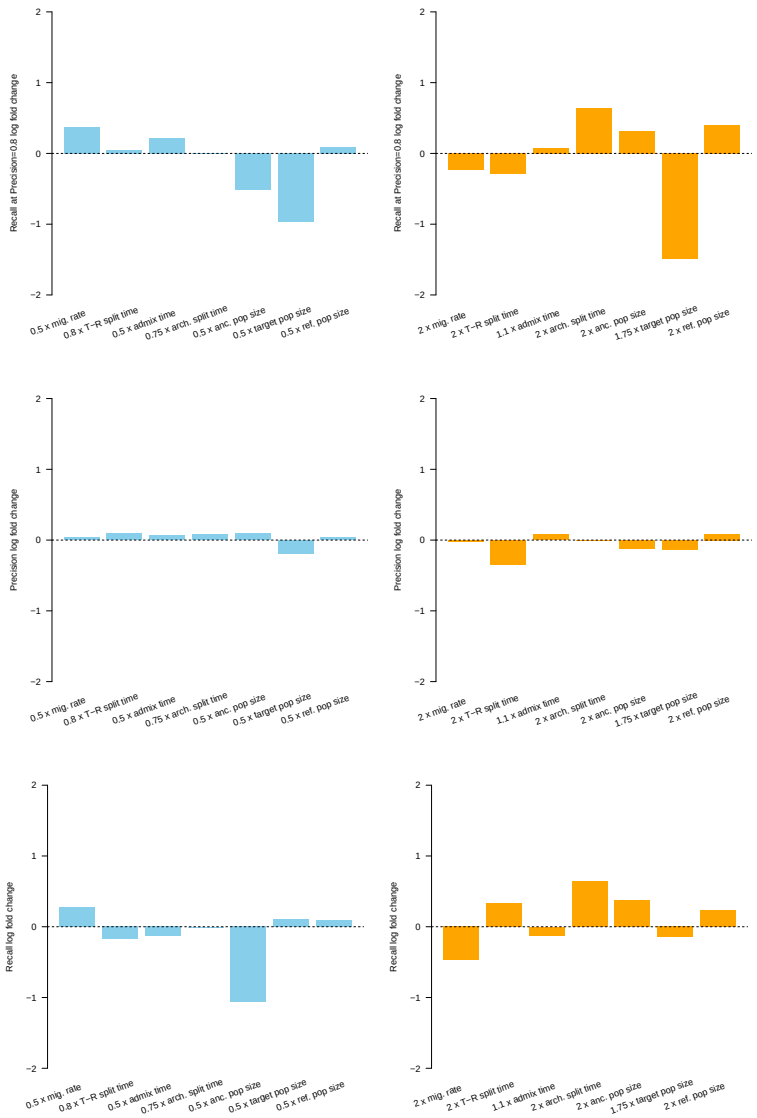

decrease. Thus there are more simulations in the unperturbed training data that contain samples that are similar to the 0.5X than to the 2X.

Recently, Hsieh *et al* [15] used a demographic model estimated from data to infer archaic admixture in African Pygmy populations. They modeled gene flow from an archaic human population that split off 24,137 generations ago into a Pygmy population 5,344 generations ago at a frequency of 2%.

In addition to the perturbations we performed here, we wanted to see how ArchIE would perform under an alternative model unrelated to what it had been trained on. Importantly, this model contains many different values across all parameter changes, which provides a different test than systematically perturbing single parameters. We simulated data under the Hsieh *et al* model and found that at the 80% precision threshold, ArchIE attained a precision of 0.998 and a recall of 0.700. This high performance is partly due to the fact that under this demographic model, the archaic split time is nearly double that of the Human-Neanderthal split time, allowing additional time for the archaic and modern human lineages to differentiate.

## ArchIE detects Neaderthal introgression in European genomes

To validate our method on a realistic setting, we applied our method to data from Phase 3 of the 1000 Genomes Project[20] to detect regions of Neanderthal introgression in the European populations without using any of the Neanderthal genomes [6, 10, 27]. We compared our inferences to results from a previous method that inferred Neanderthal ancestry using the high-coverage Altai Neanderthal genome as a reference[10] and trained on data simulated under a demographic model with parameters described in [2].

We randomly selected 50 individuals from a European (CEU) population as our target individuals and 50 individuals from an African (YRI) population as a reference and calculated the summary statistics described above. We evaluated the average percent of windows inferred as archaic as a function of the calling threshold (Figure 5A). On average, we inferred 1.99% (jackknife SE= 0.3%) of the genome as archaic at a precision of 0.8 ($P$(archaic)= 0.862) of the genome as archaic, which is in line with proportion of Neanderthal ancestry from previous analyses [2, 6, 10].

Next, we sought to determine whether the archaic haplotypes inferred by our model are enriched for introgressed Neanderthal variants. For each 50 kb window, we computed a Neanderthal match statistic

Figure 5: **Application of ArchIE to 1000 Genomes European (CEU)**. (A) Percentage of genome called archaic as a function of probability threshold. (B) Neanderthal match statistic for haplotypes inferred as archaic vs non-archaic. (C) Frequency of haplotypes labeled as archaic near *BNC2* gene and (D) the *OAS* gene cluster. (E) Mean frequency of archaic ancestry increases with B-statistic. A B-statistic near 0 denotes more selectively constrained regions. Lines indicate standard error of the mean.

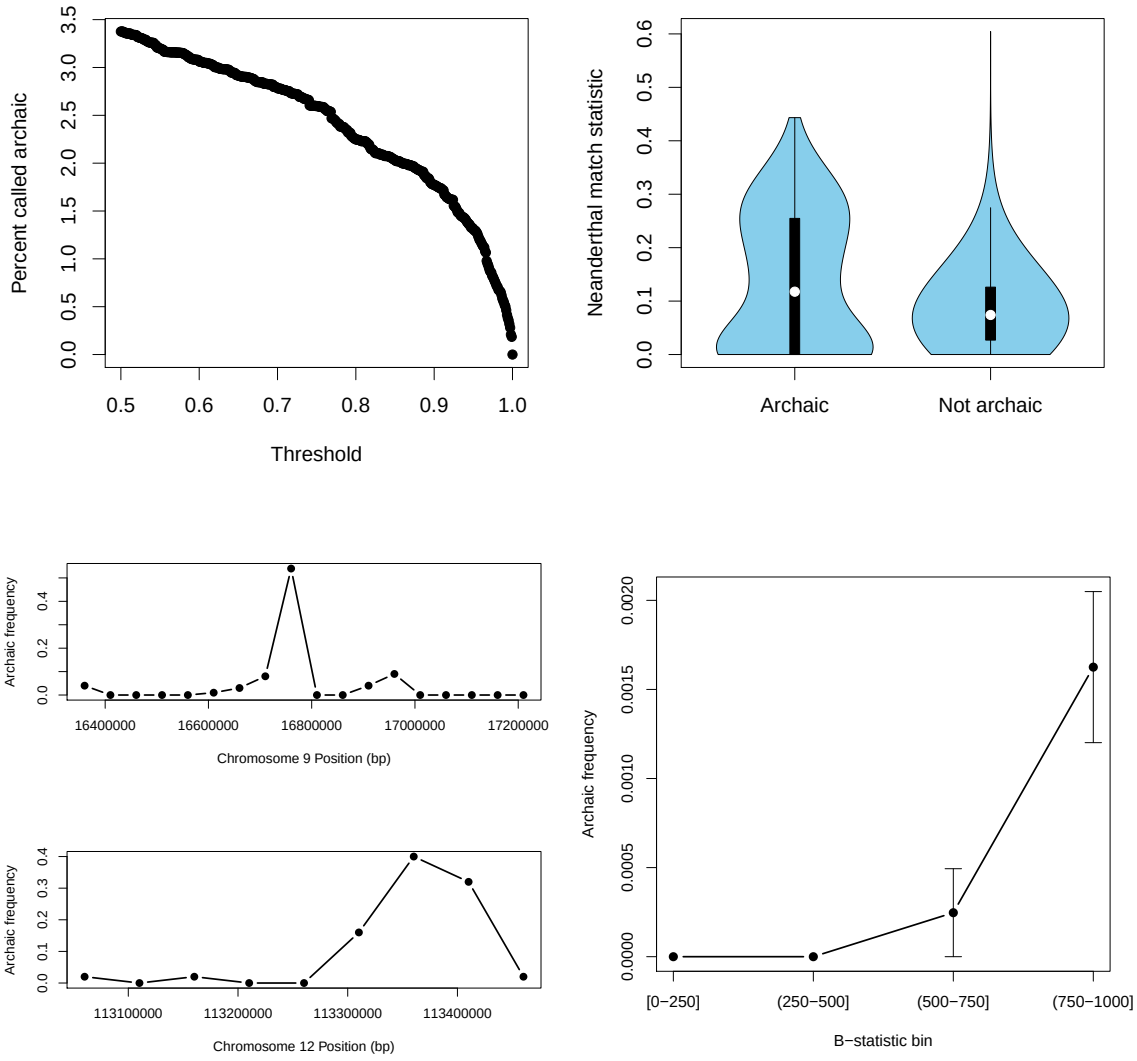

(NMS) as the number of shared variants between an individual haplotype and the Altai Neanderthal reference genome sequence [10] divided by the total number of segregating sites in that window. We see that the archaic regions confidently inferred by our method (P(archaic) $\geq 99.99\%$) have a higher NMS suggesting that, even in the absence of a reference genome, the archaic ancestry segments identified by the classifier are likely to represent introgressed Neanderthal sequence (Figure 5B; $P$ value $= 1.87 \times 10^{-11}$ via block jackknife).

We then focused on two genomic regions at which the frequency of Neanderthal ancestry in European individuals has been found to be relatively high: the *BNC2* gene (Chromosome 9:16,409,501-16,870,786) [2] and the *OAS* gene cluster (Chromosome 12:113,344,739-113,357,712) [7]. The frequency of confidently inferred archaic ancestry is substantially increased in both these genes (Figure 5C, D).

Finally, we analyzed the correlation between a measure of selective constraint of a given genomic region (B-value [19]) and frequency of confidently inferred archaic segments in the CEU population in the same region. Sankararaman *et al.* 2014 [2] describe a relationship where more constrained regions (lower B-value) have a lower frequency of archaic ancestry. We observe the same trend where more neutral regions (B-value $\geq 750$) contain more archaic ancestry than constrained regions (B-value $\leq 250$), consistent with selection against the archaic ancestry ($P$ value $= 8.49 \times 10^{-4}$ via block jackknife; Figure 5E).

These analyses suggest that ArchIE obtains results concordant with those from a previous reference-aware method indicating that the inferences from ArchIE are reasonable. We caution, however, that the observed concordance can be inflated due to any biases shared by the two methods.

## Ghost admixture into the Yoruba

We next turned our attention to inferring archaic ancestry across the genomes of 50 Yoruban individuals (YRI) from the 1000 Genomes Project [20]. We set the CEU population as the MH reference population and inferred archaic ancestry in 50KB windows. We applied the logistic regression predictor trained using the parameters from the modern Human-Neanderthal demography. While this predictor is likely to be most accurate if the introgressing archaic population had a similar relationship to the Yoruba as the Neanderthals to the CEU, we expect the predictor to be sensitive to introgression events from populations that diverged from the ancestors of the Yoruba before the YRI-CEU split and then introgressed after. We found that at a

precision of 0.8 ($P$(archaic)= 0.862), 7.97% (jackknife SE= 0.6%) of the genome is inferred to harbor archaic ancestry on average.

To understand the source of archaic ancestry in the Yoruba, we first computed a Neanderthal Match Statistic as before and and found a significant enrichment of Neanderthal matching windows (Figure 6B, $P$ value $= 5.87 \times 10^{-37}$ via block jackknife). It is plausible that this archaic ancestry is, at least partly, the result of Neanderthal introgression into the Yoruba mediated by more recent west Eurasian gene flow into Yoruba [10]. However, the proportion of Neanderthal ancestry in Yoruba is very small (about $2 \times 10^{-4}$) [10] so that we would not expect this small proportion to explain our signal.

Another potential explanation for this archaic signal is the result of admixture with an extant but highly-diverged African population. Recent studies have provided evidence for recent gene flow between Yoruba and western Central African Pygmy populations[15]. To test the hypothesis that the archaic ancestry is due to admixture with an ancestral population related to present-day Pygmy populations, we ran a similar matching statistic using a genome from the Biaka Pygmy as the reference (Figure 6C). While there is much more matching in non-archaic haplotypes, consistent with a more recent divergence, there is a depletion of matching with archaic haplotypes suggesting that the Biaka are not the source of admixture ($P$ value $= 3.23 \times 10^{-16}$ via block jackknife). Thus, the source of archaic ancestry in the Yoruba does not appear to be well-represented by extant populations.

## The genomic distribution of archaic ancestry in the Yoruba

We examined the relationship between B-value and archaic frequency to test where selectively constrained regions are less likely to contain archaic ancestry. More constrained regions (B-value $\leq 250$) harbor less archaic ancestry than more neutrally evolving regions (B-value $\geq 750$) ($P$ value $= 3.01 \times 10^{-9}$ via block jackknife; Figure 6D) indicating that archaic alleles that introgressed into the Yoruban population were deleterious on average.

On the other hand, we also find evidence for loci at which the introgressed archaic alleles are segregating at substantially elevated frequencies with 2.1 MB of introgressed sequence at high-frequency ($\geq 50\%$) and 258 MB of introgressed sequence total (Figure 8). Previous studies [9, 28] found evidence for introgres-

Figure 6: **Application of ArchIE to 1000 Genomes Yoruba (YRI)**. (A) Average percentage of genome called archaic as a function of calling threshold for 50 Yoruban individuals. (B) Neanderthal match statistics for archaic regions and non archaic called in Yoruba. (C) Pygmy match statistic for archaic and non archaic regions in Yoruba. (D) B-value versus archaic ancestry frequency. Lines indicate standard error of the mean.

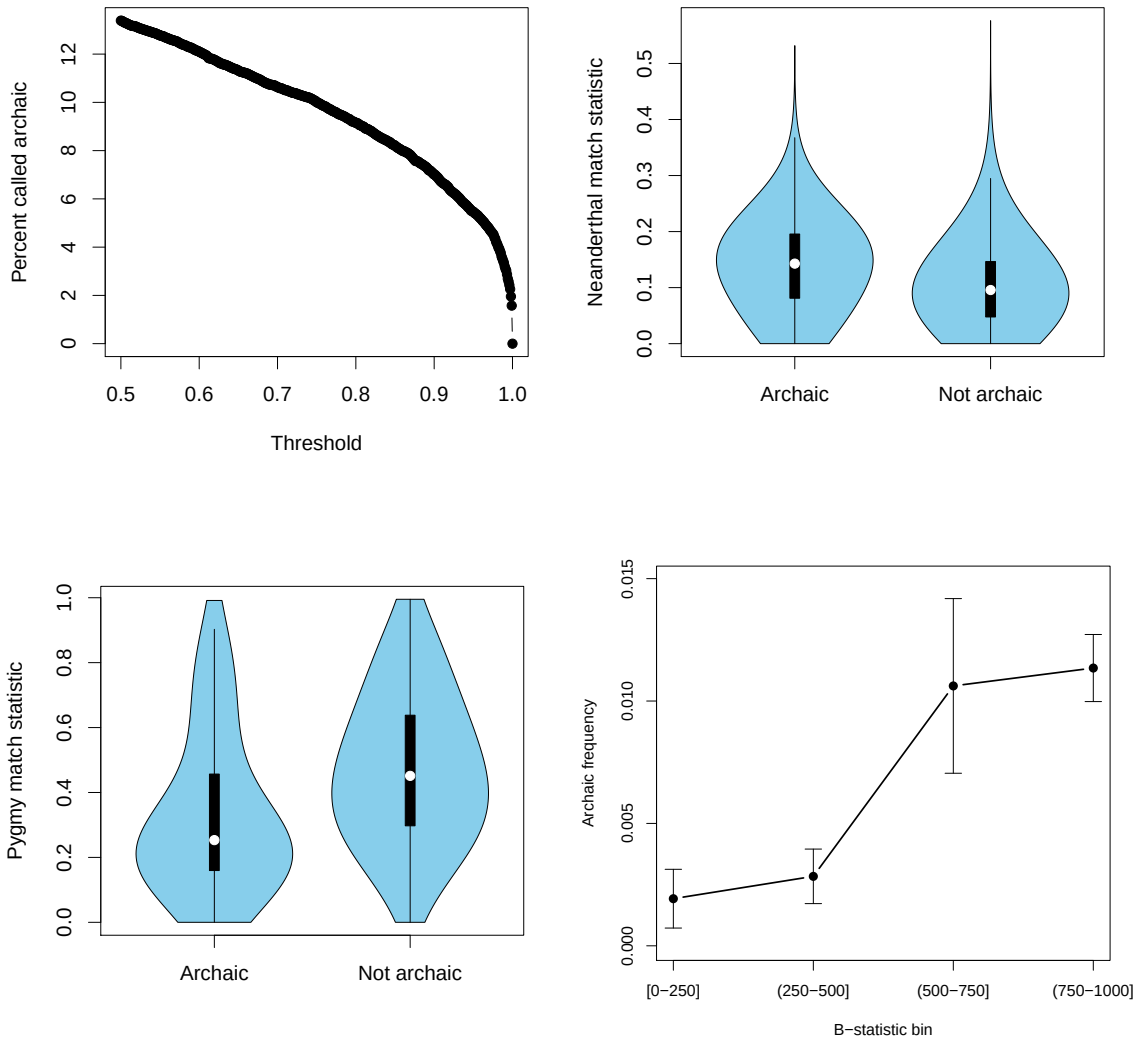

sion into Yoruban individuals using the S*-statistic on 135 loci in 12 individuals. Based on this limited data, they found evidence for introgression in several genes. We used our map of archaic introgression in the Yoruba to confirm their top three hits (ranked by *P*-value), *XRCC4* (Chromosome 5:82,373,317-82,649,579), *TJP1* (Chromosome 15:29,992,338-30,261,038), *DUT* (Chromosome 15:48,623,215-48,635,570) (Figure 7), validating their results. Further, we found several genes at high frequency including *NF1*, a tumor suppresor gene, *HSD17B2*, a gene involved with hormone regulation, and *KCNIP4*, which is a gene involved with potassium channels (Table 1). We also find genes coding for a transcription factor and an miRNA, suggesting a role for transcription regulation in these introgressed genes. Of the genes where the archaic haplotype is at high frequency, several have been found in previous scans for positive selection in the Yoruban population, including *NF1* [29, 30], *KCNIP4* [31], and *TRPS1* [32].

Taken together, these results suggest that introgression from one or more deeply diverged populations has shaped the genomes of a modern human population in Africa. Further, we find that natural selection has altered the frequency of these introgressed haplotypes, suggesting there are possible functional impacts of this introgression.

| Chromosome | Gene name | Frequency | Gene type |
|---|---|---|---|
| chr17 | *KRT18P61* | 0.84 | pseudogene |
| chr1 | *RP11-286M16* | 0.84 | lincRNA |
| chr17 | *NF1* | 0.83 | protein coding |
| chr21 | *MIR125B2* | 0.76 | miRNA |
| chr16 | *HSD17B2* | 0.74 | protein coding |
| chr1 | *RN7SKP160* | 0.74 | pseudogene |
| chr4 | *KCNIP4* | 0.73 | protein coding |
| chr8 | *TRPS1* | 0.71 | protein coding |
| chr17 | *RP1115E18* | 0.67 | pseudogene |
| chr6 | *MTFR2* | 0.67 | protein coding |

Table 1: **Genomics regions with a high frequency of archaic ancestry in the Yoruba**.

Figure 7: **Validation of previously found genes suggestive of archaic introgression [9]**. Top to bottom: *XRCC4*, *TJP1*, *DUT*.

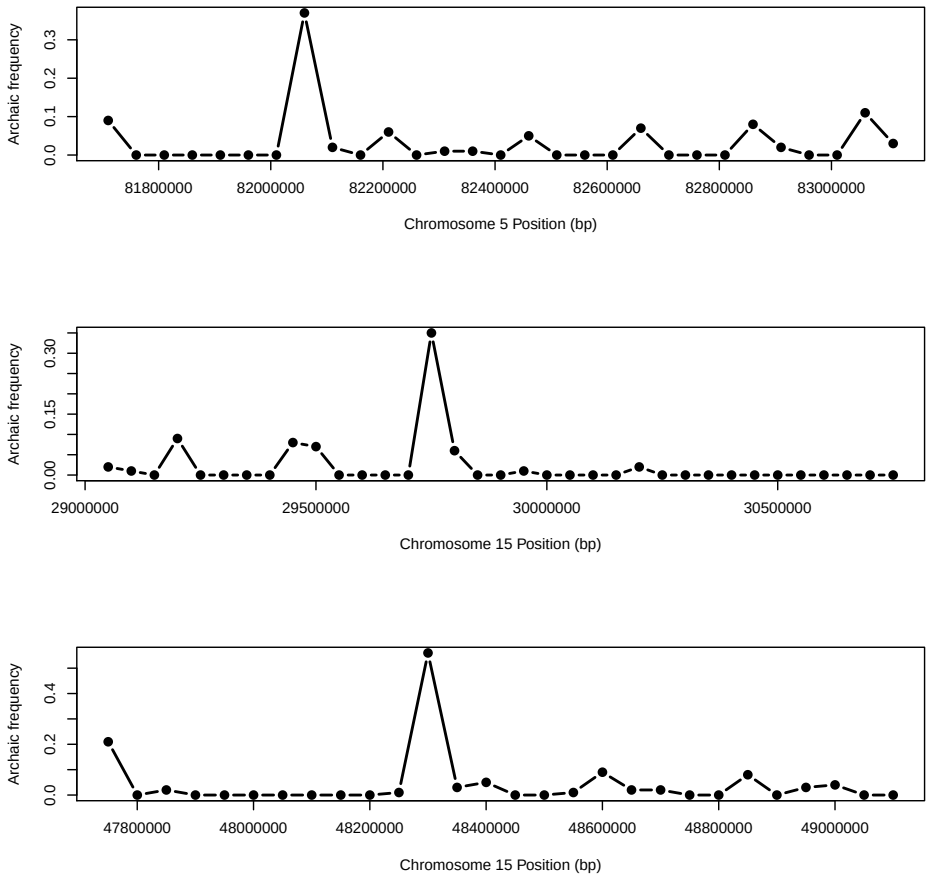

Figure 8: **Genome wide map of archaic ancestry in Yoruba**. Y-axis denotes the frequency of archaic haplotypes.

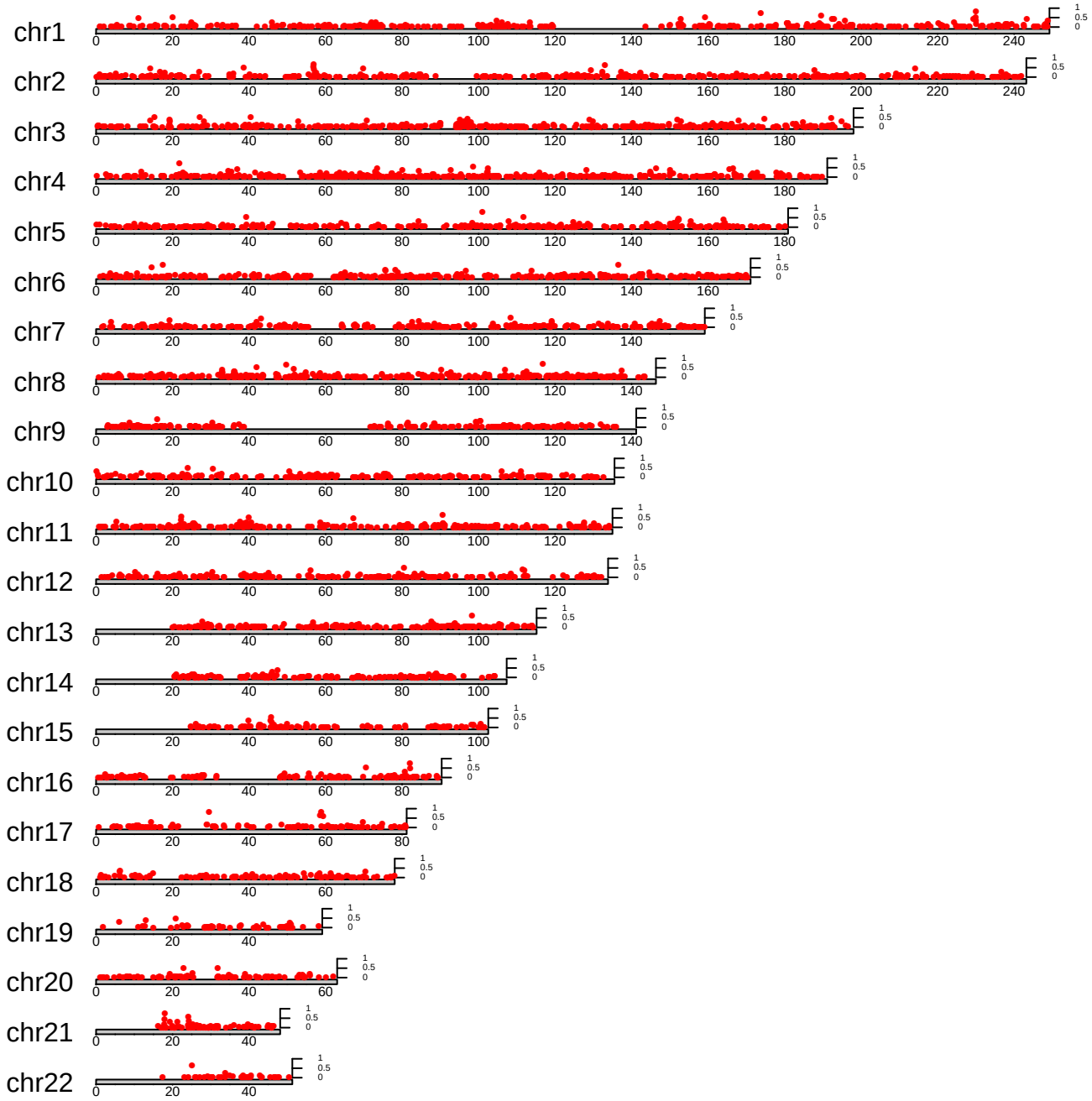

# Discussion

Detecting archaic admixture and characterizing its impact on genetic variation is an important problem in human population genetics. Here, we present a classification approach to detecting regions of archaic local ancestry without the need for an archaic reference sequence. Our method combines weakly informative signals across a wide range of statistics to create a more powerful predictor.

Our results suggest that Yoruban individuals trace about 7.9% of their genomes to an as yet unidentified archaic population. This is in agreement with some results from previous papers in other African populations such as the Biaka and the Baka [15], suggesting that there was a rich diversity of hominin species within Africa and that introgression was commonplace. Using our inferred segments of archaic ancestry in the Yoruba, we find that there are regions of the genome that are under higher selective constraint have reduced archaic ancestry on average indicating that the archaic alleles were deleterious in the hybrid population. More data is needed for a complete picture of these ghost populations. For example, it is unclear whether the archaic signatures found here are from the same as those found in other African populations[13, 14, 15, 33].

One advantage of our approach is that the learning algorithm is general allowing it to be applied broadly to diverse prediction problems as well as input features while its simplicity allows for a transparent interpretation of the features and the model. It is possible for us to examine the weights and determine the relative contribution the algorithm learns to place on each feature. In doing so, we find that there is moderate weight on each value of the individual frequency spectrum and more weight is placed on the skew of the distance vector, the number of private SNPs, and the minimum distance to the MH reference.

There are several future directions we propose based off these results. First, it is possible to train more complex models like deep neural networks, which can learn and capture non-linear relationships between features and tend not to suffer from the curse of dimensionality [16]. These methods have been used to great success in tasks such as image classification [34] and we anticipate their use in population genetics could improve predictive power. Preliminary results applying deep learning to this problem with the features used here are promising, motivating future work. A related direction could be to automatically learn features from raw sequencing data. Our method relies on hand crafted features that are informed by population genetics theory, similar to other methods that have been proposed in population genetics [16, 17, 35, 36].

In conclusion, our method improves on previous methods for reference-free inference of archaic ancestry by combining informative summary statistics in a statistical learning framework. We anticipate that this method will be informative not only in human populations where questions about admixture with other hominins abound, but also in other species and systems where pervasive admixture has shaped the distribution of genetic variation.

# Methods

## Simulating training data

We simulated training and test data sets using a modified version of ms [21] that tracks ancestry of each site in each individual genome. Using a previously proposed demographic model relating modern humans and Neanderthals [2], we sampled 100 haplotypes from from population 2 (the target), and 100 haplotypes from population 1 (MH reference) over a region of length 50 kb. We use a mutation rate $\mu = 1.25 \times 10^{-8}$ and a recombination rate $r = 1 \times 10^{-8}$. This was used as training data for both the CEU-Neanderthal introgression inference and the YRI-Ghost introgression inference.

The general demography is as follows: a population of size $N_a$ splits from a population of size $N_0$ $T_0$ generations ago. Then, at $T_S$, two populations split off from the ancestral population that are size $N_1$ and $N_2$. Then, at time $T_A$, the archaic population migrates into $P_2$ with a rate of $m$. See Figure 1A for a graphical outline.

## Feature calculation

Each simulation at a given locus generates 100 haplotypes in the target population. For each haplotype, we calculate the following classes of summary statistics: haplotype level frequency spectrum, distance vector to all haplotypes within the test population, minimum distance to haplotypes in population 1, the number of private SNPs, and the S*-statistic.

The individual frequency spectrum is created as follows: given a sample of $n$ haplotypes, for each haplotype $j$, we construct a vector $X$ of length $n$ where entry $X_i$ counts the number of derived alleles in the

focal haplotype $j$ at frequency $i$. For example, the first entry counts the number of singletons present in the haplotype, the second entry counts the number of doubletons and so on until $n$.

The distance vector is a vector of length $n$ where each entry is the Euclidean distance from haplotype $x$ to haplotype $y_i$ over all sites, where $x$ is the focal haplotype and $y_i$ is the haplotype being compared.

This results in 208 features per example (a 50kb window for a single haploid genome), with 100 examples per locus and 10,000 loci resulting in 1,000,000 examples for training before filtering haplotypes with intermediate levels of admixture.

## Learning algorithm

We tested the ability of a logistic regression framework to classify archaic ancestry from non-archaic ancestry. We used the "glm" function in R to construct a logistic model using the family=binomial("logit") option. We used the predict function to obtain a prediction and converted it to a probability using the "plogis" function.

We evaluated the performance using Precision-Recall (PR) curves. We calculated precision and recall as:

$$Recall(t) = \frac{TP(t)}{TP(t) + FN(t)}$$
$$Precision(t) = \frac{TP(t)}{TP(t) + FP(t)}$$

Where $TP(t)$ is the number of true positives at threshold $t$, $FN(t)$ is the number of false negatives at threshold $t$, and $FP(t)$ is the number of false positives at threshold $t$. In this case, a true positive is a haplotype that traces ancestry back to the archaic population that we call as archaic. A false negative is a haplotype that also traces ancestry back to the archaic population, but does not pass our threshold for calling archaic. A false positive is a haplotype that passes our threshold for being called archaic, but traces its ancestry back to the target population rather than the archaic population.

## Robustness

We examined the robustness of ArchIE to a specified demographic model by systematically perturbing one parameter at a time, simulating a dataset, and evaluating ArchIE's performance. We doubled and halved

the parameters, except when doing so would produce a demographic model that is not sensible.

## Neanderthal introgression

We validated our method using the Neanderthal introgression scenario as a test case. We downloaded phased CEU genomes from the 1000 Genomes Phase 3 dataset [20] and calculated the features mentioned above in 50KB windows. For each individual haplotype, we inferred the probability that the window is archaic. We then intersected our calls with the 1000 Genomes strict mask using BEDtools v2.26.0 [37], removing regions that are difficult to map to.

We calculated a Neanderthal match statistic (NMS) for focal haplotype $i$ as the number of segregating sites in a window shared with the Altai Neanderthal [10] genome:

$$NMS_i = \frac{S_i}{N_i + H_i}$$

where $S_i$ denotes the number of segregating sites between the focal haplotype and the Neanderthal genome, $N_i$ denotes the number of Neanderthal segregating sites, and $H_i$ denotes the number of human segregating sites. Since the Neanderthal genome is not phased, we counted a site as matching if it contained at least one single matching allele or more. We dropped sites with missing data in the Altai reference genome.

We tested for significant differences between windows we call archaic and non archaic using a 1 megabase (MB) block jackknife. For each window, we compute the mean NMS for archaic and non archaic haplotypes, take the difference, and then divide by the ungrouped mean NMS to control for mutation rate heterogeneity. To compute significance, we drop 1 MB windows (non-overlapping) and recalculate the genome wide difference in means.

## Background selection

In order to assess the relationship between background selection and inferred archaic ancestry, we use the B-values from McVicker *et al.* 2009 [19] and intersected them with our calls. For visualization, we binned the B-values into 4 bins, [0-250], (250-500], (500-750], and (750-1000].

We tested for significant differences in allele frequency between the lowest and highest bins using a block jackknife, dropping each window and recalculating the difference in allele frequency.

### Ghost admixture

We evaluated the presence of ghost admixture into the Yoruba population by sampling 50 individuals from the 1000 Genomes project phase 3 data set [20]. As before, we calculated features in 50 KB windows, intersected the calls with the 1000 Genomes strict mask, this time using the CEU population as the MH reference. We calculated NMS on confidently archaic and non archaic haplotypes as above and calculated a Pygmy match statistic (PMS) using a single Biaka genome as the reference [1].

## Acknowledgements

We would like to thank Emilia Huerta Sánchez and Benjamin Vernot for help with S*, members of the Lohmueller and Sankararaman labs, the UCLA Medical and Population Genetics group for helpful discussions, and Alec Chiu for comments on a draft of the paper. SS is supported in part by NIH grants R00GM111744, R35GM125055, an Alfred P. Sloan Research Fellowship, and a gift from the Okawa Foundation.

## References

[1] Mallick, S. *et al.* The Simons Genome Diversity Project: 300 genomes from 142 diverse populations. *Nature* **538**, 201 (2016). URL `https://www.nature.com/articles/nature18964`.

[2] Sankararaman, S. *et al.* The genomic landscape of Neanderthal ancestry in present-day humans. *Nature* **507**, 354–357 (2014). URL `https://www.nature.com/nature/journal/v507/n7492/full/nature12961.html`.

[3] Vernot, B. & Akey, J. M. Resurrecting Surviving Neandertal Lineages from Modern Human Genomes. *Science* **343**, 1017–1021 (2014). URL `http://science.sciencemag.org/content/343/6174/1017`.

[4] Simonti, C. N. *et al.* The phenotypic legacy of admixture between modern humans and Neandertals. *Science* **351**, 737–741 (2016). URL http://science.sciencemag.org/content/351/6274/737.

[5] McCoy, R. C., Wakefield, J. & Akey, J. M. Impacts of Neanderthal-Introgressed Sequences on the Landscape of Human Gene Expression. *Cell* **168**, 916–927.e12 (2017). URL http://www.sciencedirect.com/science/article/pii/S0092867417301289.

[6] Green, R. E. *et al.* A Draft Sequence of the Neandertal Genome. *Science* **328**, 710–722 (2010). URL http://science.sciencemag.org/content/328/5979/710.

[7] Mendez, F. L., Watkins, J. C. & Hammer, M. F. Neandertal origin of genetic variation at the cluster of OAS immunity genes. *Molecular Biology and Evolution* **30**, 798–801 (2013).

[8] Patterson, N. *et al.* Ancient admixture in human history. *Genetics* **192**, 1065–1093 (2012).

[9] Plagnol, V. & Wall, J. D. Possible Ancestral Structure in Human Populations. *PLOS Genetics* **2**, e105 (2006). URL http://journals.plos.org/plosgenetics/article?id=10.1371/journal.pgen.0020105.

[10] Prüfer, K. *et al.* The complete genome sequence of a Neanderthal from the Altai Mountains. *Nature* **505**, 43–49 (2014). URL http://www.nature.com/nature/journal/v505/n7481/abs/nature12886.html.

[11] Seguin-Orlando, A. *et al.* Genomic structure in Europeans dating back at least 36,200 years. *Science* **346**, 1113–1118 (2014). URL http://science.sciencemag.org/content/346/6213/1113.

[12] Reich, D. *et al.* Genetic history of an archaic hominin group from Denisova Cave in Siberia. *Nature* **468**, 1053–1060 (2010).

[13] Hammer, M. F., Woerner, A. E., Mendez, F. L., Watkins, J. C. & Wall, J. D. Genetic evidence for archaic admixture in Africa. *Proceedings of the National Academy of Sciences* **108**, 15123–15128 (2011). URL http://www.pnas.org/content/108/37/15123.

[14] Lachance, J. *et al.* Evolutionary History and Adaptation from High-Coverage Whole-Genome Sequences of Diverse African Hunter-Gatherers. *Cell* **150**, 457–469 (2012). URL http://www.cell.com/cell/abstract/S0092-8674(12)00831-8.

[15] Hsieh, P. *et al.* Model-based analyses of whole-genome data reveal a complex evolutionary history involving archaic introgression in Central African Pygmies. *Genome Research* (2016). URL http://genome.cshlp.org/content/early/2016/02/08/gr.196634.115.

[16] Sheehan, S. & Song, Y. S. Deep Learning for Population Genetic Inference. *PLOS Computational Biology* **12**, e1004845 (2016). URL http://journals.plos.org/ploscompbiol/article?id=10.1371/journal.pcbi.1004845.

[17] Schrider, D. R. & Kern, A. D. S/HIC: Robust Identification of Soft and Hard Sweeps Using Machine Learning. *PLOS Genetics* **12**, e1005928 (2016). URL http://journals.plos.org/plosgenetics/article?id=10.1371/journal.pgen.1005928.

[18] Schrider, D., Ayroles, J., Matute, D. R. & Kern, A. D. Supervised machine learning reveals introgressed loci in the genomes of Drosophila simulans and D. sechellia. *bioRxiv* 170670 (2017). URL https://www.biorxiv.org/content/early/2017/09/25/170670.

[19] McVicker, G., Gordon, D., Davis, C. & Green, P. Widespread Genomic Signatures of Natural Selection in Hominid Evolution. *PLOS Genetics* **5**, e1000471 (2009). URL http://journals.plos.org/plosgenetics/article?id=10.1371/journal.pgen.1000471.

[20] The 1000 Genomes Project Consortium. A global reference for human genetic variation. *Nature* **526**, 68–74 (2015). URL https://www.nature.com/nature/journal/v526/n7571/full/nature15393.html.

[21] Hudson, R. R. Generating samples under a Wright–Fisher neutral model of genetic variation. *Bioinformatics* **18**, 337–338 (2002). URL https://academic.oup.com/bioinformatics/article/18/2/337/225783.

[22] Heerwaarden, J. v. *et al.* Genetic signals of origin, spread, and introgression in a large sample of maize landraces. *Proceedings of the National Academy of Sciences* **108**, 1088–1092 (2011). URL http://www.pnas.org/content/108/3/1088.

[23] Hufford, M. B. *et al.* The Genomic Signature of Crop-Wild Introgression in Maize. *PLOS Genetics* **9**, e1003477 (2013). URL http://journals.plos.org/plosgenetics/article?id=10.1371/journal.pgen.1003477.

[24] Brandvain, Y., Kenney, A. M., Flagel, L., Coop, G. & Sweigart, A. L. Speciation and Introgression between Mimulus nasutus and Mimulus guttatus. *PLOS Genetics* **10**, e1004410 (2014). URL http://journals.plos.org/plosgenetics/article?id=10.1371/journal.pgen.1004410.

[25] Novikova, P. Y. *et al.* Sequencing of the genus Arabidopsis identifies a complex history of nonbifurcating speciation and abundant trans-specific polymorphism. *Nature Genetics* **48**, 1077–1082 (2016). URL https://www.nature.com/ng/journal/v48/n9/full/ng.3617.html.

[26] Kryvokhyzha, D. *et al.* Parental legacy, demography, and introgression influenced the evolution of the two subgenomes of the tetraploid Capsella bursa-pastoris (Brassicaceae). *bioRxiv* 234096 (2017). URL https://www.biorxiv.org/content/early/2017/12/13/234096.

[27] Meyer, M. *et al.* A High-Coverage Genome Sequence from an Archaic Denisovan Individual. *Science* **338**, 222–226 (2012). URL http://science.sciencemag.org/content/338/6104/222.

[28] Wall, J. D., Lohmueller, K. E. & Plagnol, V. Detecting Ancient Admixture and Estimating Demographic Parameters in Multiple Human Populations. *Molecular Biology and Evolution* **26**, 1823–1827 (2009). URL http://www.ncbi.nlm.nih.gov/pmc/articles/PMC2734152/.

[29] Kudaravalli, S., Veyrieras, J.-B., Stranger, B. E., Dermitzakis, E. T. & Pritchard, J. K. Gene expression levels are a target of recent natural selection in the human genome. *Molecular Biology and Evolution* **26**, 649–658 (2009).

[30] Grossman, S. R. *et al.* Identifying recent adaptations in large-scale genomic data. *Cell* **152**, 703–713 (2013).

[31] International HapMap Consortium *et al.* A second generation human haplotype map of over 3.1 million SNPs. *Nature* **449**, 851–861 (2007).

[32] Barreiro, L. B., Laval, G., Quach, H., Patin, E. & Quintana-Murci, L. Natural selection has driven population differentiation in modern humans. *Nature Genetics* **40**, 340–345 (2008). URL https://www.nature.com/articles/ng.78.

[33] Xu, D. *et al.* Archaic Hominin Introgression in Africa Contributes to Functional Salivary MUC7 Genetic Variation. *Molecular Biology and Evolution* **34**, 2704–2715 (2017). URL https://academic.oup.com/mbe/article/34/10/2704/3988100.

[34] LeCun, Y., Bengio, Y. & Hinton, G. Deep learning. *Nature* **521**, 436–444 (2015). URL http://www.nature.com/nature/journal/v521/n7553/full/nature14539.html.

[35] Schrider, D. R. & Kern, A. D. Machine Learning for Population Genetics: A New Paradigm. *bioRxiv* 206482 (2017). URL https://www.biorxiv.org/content/early/2017/10/20/206482.

[36] Chan, J. *et al.* A Likelihood-Free Inference Framework for Population Genetic Data using Exchangeable Neural Networks. *bioRxiv* 267211 (2018). URL https://www.biorxiv.org/content/early/2018/02/18/267211.

[37] Quinlan, A. R. & Hall, I. M. BEDTools: a flexible suite of utilities for comparing genomic features. *Bioinformatics* **26**, 841–842 (2010). URL https://academic.oup.com/bioinformatics/article/26/6/841/244688.